

HEAT-MASS TRANSFER IN SUPERSONIC CHEMICAL LASERS**A.S. Boreysho, V.M. Malkov, A.V. Savin***Laser Systems Ltd., Baltic State Technical University
Saint-Petersburg, Russia*

Supersonic chemical lasers remain the most powerful CW sources of high-quality powerful coherent radiation. The provision of their operation and the obtaining of estimated characteristics are linked inseparably with the solving of many heat-mass transfer problems in regard to complicated interacting gas and liquid flows in real constructions. Such problems arise at all the stages of laser's operation and practically in all its units and subsystems.

Active medium (AM) of high-efficient chemical lasers (CL) represents a supersonic chemically-reacting flow of gas mixture. Therefore, key laser parameters of the medium are determined by gas dynamic processes. Parameters like the small signal gain (SSG), saturation intensity, specific laser energy reduced to unit weight of the medium, as well as recovered pressure and total flow rate depend on the heat-mass transfer and fluid dynamic operational mode. Therefore, a lot of efforts aimed at investigation of CL heat-mass transfer and fluid dynamics are already spent and also many issues remain unclear and should be investigated additionally.

Similarity of CL AM flows is determined by usual gas-dynamic criteria – Mach number (M) and Reynolds number (Re) - as well as more special criteria – Damkeller number (Da) and thermal factor (Θ). Damkeller number is used for characterization of chemical mode of the active medium (AM) flows and generally represents a ratio of a chemical characteristic time to a gas-dynamic convection time. Certainly different chemical processes have different characteristic times, but chemical processes responsible for the heat release are the most important from gas-dynamic viewpoint. Thermal factor is used for characterization of thermodynamic mode of the AM flow and represents a ratio of the residual energy of the AM (the part of inversed-population energy not converted to the laser radiation) to the translational total enthalpy. In case of COIL - the most promising CL – there are two main features of CL AM flows distinguishing them from usual gas-dynamic flows:

Chemical characteristic time is long enough because the processes mainly responsible for the heat release are slow. On the contrary, convective gas-dynamic time in a supersonic COIL is short because of big downstream velocity. Therefore, Damkeller number for supersonic COIL AM flows is large enough. Quantitatively, assuming that the main heat source in the resonator cavity flow is the quenching of excited iodine atoms $I^* + H_2O \xrightarrow{k_{26}} I + H_2O$, and supposing perfect equilibrium in very fast pumping reaction $I + O_2(^1\Delta) \rightarrow I^* + O_2(^3\Sigma)$, it can be easily shown that time of $[O_2(^1\Delta)]$ half-decay $\tau_{1/2}$:

$$\tau_{1/2} = \left(\frac{Y_0}{2} + \frac{1 + \frac{k_{26} w}{k_b}}{K_{eq} - 1} \ln 2 \right) / \left(\frac{K_{eq}}{K_{eq} - 1} k_{26} [I_\Sigma] w \right), \quad (1)$$

where “w” is reduced water vapor concentration. For typical supersonic COIL this time is $\sim 10^{-4}$ s. Gas-dynamic downstream-convection time for supersonic COIL ($\tau_{conv} = L/U$) also has the similar order of magnitude. Therefore, $Da \sim 1$ – in contrast to HF/DF lasers where similar Da is one-two orders less.

Residual chemical energy not converted to the laser radiation for COIL AM is much higher than the total translational enthalpy because of high energy efficiency as well as low total temperature of the AM. The corresponding thermal factor for nitrogen-based COIL can be estimated as (2), where Y_{res} is residual yield and D means dilution ratio. For typical COIL parameters $\theta \sim 1.5 \div 2$, as distinct from HF/DF lasers where the thermal factor is much closer to 1.

$$\theta = 1 + \frac{\gamma - 1}{\gamma} \frac{hc}{k \lambda T_0} \frac{Y_{res}}{(1 + D)} \quad (2)$$

Because of two mentioned distinctions as well as low Reynolds numbers gas-dynamic processes in COIL AM represents considerable difference as compared with any other types of cw CL flows. And further, these distinctions cause main features of heat-mass transfer processes.

Laser medium component supply system:

For the most promising supersonic chemical laser – that is the oxygen-iodine laser (COIL) – the source components for the production of the laser active medium are Basic solution of Hydrogen Peroxide (BHP), liquid chlorine as well as solid iodine. All these substances are able to come into thermal and chemical interaction with constructive materials actively and also require maintenance of special conditions for the provision of their stable storage and discharge to the laser. Narrow working temperature ranges of these products require annexation of such subsystems as refrigerating units, heaters and various mixers to the system of components' preparation with a view to the conditions' stability and the maintenance of predetermined rates of heat-mass transfer processes.

Singlet Oxygen Generator - SOG:



Fig. 1. 10-kW-class COIL laser module

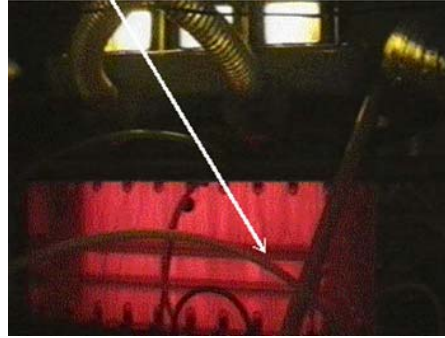


Fig. 2. The $O_2(^1\Delta)$ red emission during 0.5-mole/s SOG operation

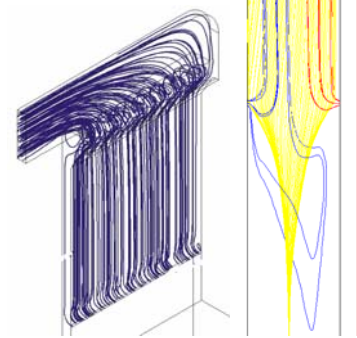


Fig. 3. 3D two-phase flow structures in SOG channel

It is the principal chemical reactor of COIL (Fig. 1 – SOG of counter-flow type). It is here where the heterogeneous chemical interaction of BHP with gaseous chlorine passes, as a result the singlet oxygen molecules are generated – this singlet oxygen is the power-producing donor of COIL. The main requirements of this device are as follow: (1) provision of high energy effectiveness $Y \times U$ (Y – singlet oxygen yield, U – degree of chlorine utilization) upon the maintenance of required heat-mass transfer characteristics during the entire period of laser's continuous work; (2) provision of minimal amount of water steam in gaseous products of SOG - $[H_2O]/[O_2]$, the perfect separation of fine-dispersed liquid droplets till the incoming of singlet oxygen to the laser nozzle bank, and maximum possible pressure of the medium P_0 ; and (3) provision of maximum rate of yield of BHP resource under the condition of heat-mass transfer processes stability. For the fulfillment of these requirements it is necessary to provide nominal gas-dynamic and heat-mass transfer regime of heterogeneous chemical interaction behavior and to prevent generation of complicated non-desirable three-dimensional structures (Fig. 2, 3). It is possible to be provided in case of SOG of the most promising counter-flow type provided that $K_f < 2000$ ($K_f = H^2 \sigma / r$ – similarity criterion of two-phase gas-dynamic processes in SOG, H – size of channel, σ – specific inter-phase surface, r – typical scale of liquid phase, droplets and/or jets).

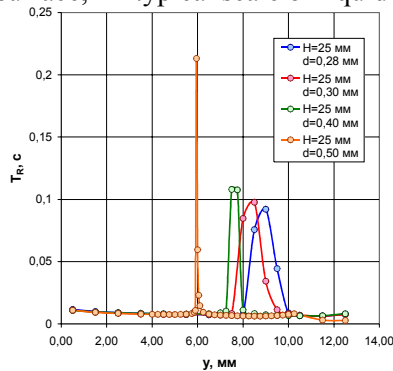


Fig. 4. Gas-phase residence time along the SOG exit cross-section.

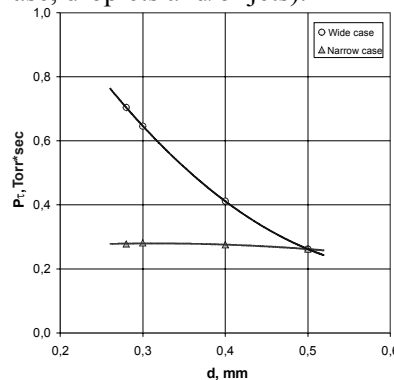


Fig. 5. Estimated $P \times \tau$ for “wide” and “narrow” cases vs. liquid particles diameter

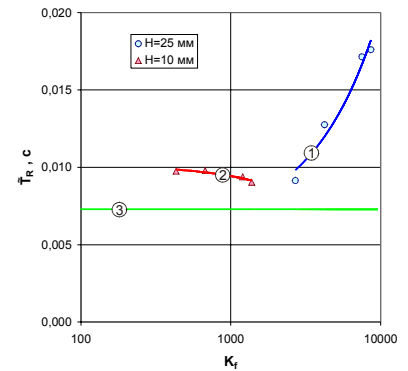


Fig.6. Gas-phase residence time vs. K_f value, 1 – ‘wide’ chamber; 2 – ‘narrow’ one; 3 – volume-averaged.

Due to strong influence of liquid-gas-phase interaction onto the mass transfer effects in reaction volume of SOG, different flow modes can appear some of which can diminish the SOG efficiency substantially. For the purpose of counter-flow disclosure the series of numerical simulation of two-phase flow in SOG were carried out. Model flow of air and water droplets was considered. The flow is considered to be iso-

thermal and laminar with monodisperse spherical droplets. Gravity was taken into account. Navier-Stokes equations were solved with CFX-5 code [8]. Two geometries were investigated – with wide (25mm) and narrow (10mm) reactionary zones. Diameter of droplets was varied. The non-structured tetrahedral grid with mesh control in heavy gradients areas was used. Total number of elements was ~250000 in both cases.

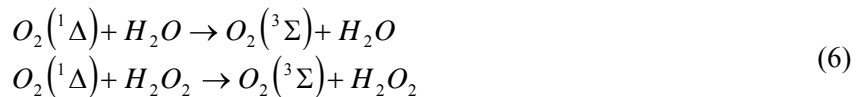
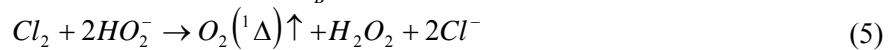
Initial conditions were set as follows: gas pressure in the reactionary chamber $P=30$ Torr, volume fraction of liquid phase $\varphi = 0.09$, velocity of droplets in Y direction $U_{jy}=-6$ m/sec. “Gas inlet” corresponds to specific molar flow rate like in [1], volume fraction of gas is 1; “liquid inlet” also corresponds to parameters of this device and $\varphi=0.09$; “liquid surface” means “wall” for gas and free output for liquid; “outlet” is a free output for both phases, $P=25$ Torr. Since calculation domain is an element of symmetry of reactionary chamber, on the frontal and on the back surfaces the “symmetry” condition was set. Other surfaces are “free-slip walls”.

As a result, gas-phase streamlines were plotted for wide and narrow geometries (see Fig 3). According 3D simulation reversed-flow mode present at $K_f > 470$ in case of wide reactionary chamber. In case of narrow reactionary chamber $K_f < 470$ and the reversed flows are absent in all variety of K_f .

An important parameter of SOG - $P \times \tau$ - was calculated, being based on the residence time τ presented on Fig 4. In case of wide reactionary chamber the exit-surface-averaged $P \times \tau$ strongly depends on droplets diameter and may be almost 3 times higher than value, which taking into account volume-averaged gas velocity \dot{V}_g / F . High $P \times \tau$ is good for chlorine utilization, but leads to high singlet oxygen losses due to its “pooling” (see eqns. (3)-(6)).

$$Ut = 1 - \exp(-\beta\sigma\tau) \quad (3)$$

$$Y = \frac{Y_0}{1 + 2k_q Y_0 Ut \frac{P}{k_B T} \tau} \quad (4)$$



Here β - mass transfer coefficient for reaction (5), for jet-type SOG typical value $\beta=70$ cm/sec; k_q – constant of “pooling” reaction (6) $k_q=2.5 \cdot 10^{-17}$ cm³/sec; Y_0 – detachment yield, in this work Y_0 is considered to be 0.94; k_B – Boltzmann constant.

Estimated values of τ and $P \times \tau$ for “wide” and “narrow” cases are shown in Fig. 5, 6. In case of “wide” reactionary chamber singlet oxygen yield drops down when droplets diameter decreases due to increasing of $P \times \tau$. In case of “narrow” reactionary chamber singlet oxygen yield is almost independent of droplets diameter, and its value close to estimated by (4) and to experimental results.

Therefore, an additionally similarity criterion for gas flow in SOG is found through self-similar solution. Two different flow modes appear with various spatial scale of velocity field depending on the value of new criterion. This is important from point of view of liquid-gas mass-transfer prediction, because this phenomena is limiting performance of SOG.

Mixing Nozzle Bank - MNB:

The formation of laser medium passes and the mixing and the interaction of singlet oxygen with gaseous iodine starts in the nozzle bank, as a result the processes of molecular iodine dissociation and the excitation of electron levels of iodine atoms pass in series.

The analysis of flows of mixing/reacting gases in small-scale supersonic nozzles requires the use of the entire contemporary tools and methods of modeling of gas-dynamic working processes of reacting mediums – equation of heterogeneous gas mixtures’ gas-dynamics, chemical and relaxation kinetics, hybrid calculating grids, high-performance calculations made on parallel clustered platforms etc. (Fig. 7-9). In view of the fact that the energy accumulated in form of excitation of molecules’ electron levels is the same order of value as the translational enthalpy of medium (i.e. temperature factor $\theta=1+Y \times [N_A h\nu] / [C_p T_0(1+D)]$ is much higher than one), the very important role is played by the heat transfer between three-dimensional flow and the nozzle construction parts.

Iodine mixer and NB flow determine the AM lasing parameters as well as potential recovered pressure, and so, the organization of iodine mixing is critical for COIL. Early numerical results [1] obtained with

RANS + $k-\omega$ SST model exhibits overestimated small signal gain (SSG). One of possible reason for this is non-stationary effects which were not taken in account in highly-symmetrical simulation. Reynolds number based on oxygen flow parameters and the injected jet size is about $10^3 \sim 10^4$, therefore large-scale self-sustained oscillations similar to transversal-cylinder Karman type flow probably can appear. In this case mixing rate will be different and the high-sensitive kinetics of the iodine dissociation will change. Simulation of such type of flow oscillations require much larger computational domain than it was used in the earlier simulations [1] because of much less symmetry in the flow. Part of such domain illustrated in Fig. 12.

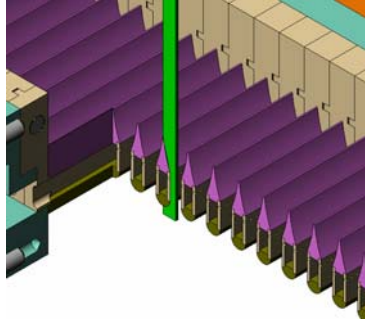


Fig. 7. COIL NB simulation model

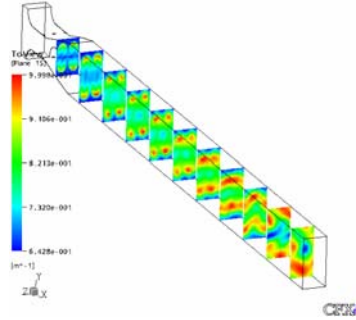


Fig. 8. 3D flow structure inside COIL NB and cavity channel illustrating mixing of O_2 (Δ) and I_2

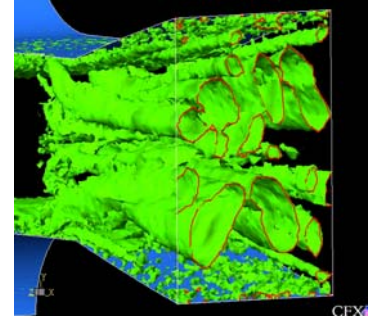


Fig. 9. 3D flow structure inside COIL NB illustrating vortex dynamics

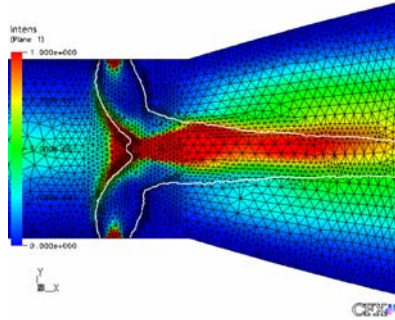


Fig. 10. Intermediate-scale computational grid illustrating the grid adaptation.

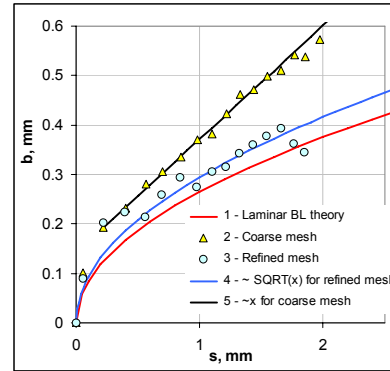


Fig. 11. Width of the upwind mixing layer of injected iodine jet; 1 – laminar theory [2]; 2, 3 – simulation; 4, 5 – power-law approximations.

The whole one includes pre-nozzle area and the laser cavity. Unstructured grid was used and 2-staged adaptation procedure was applied to obtain the final grid. The main criterion for grid-convergence procedure was the growing law of upwind shear layer of the injected jet. First, the transversally-injected supersonic jet is investigated extensively including the mixing layers [2]. Second, the initial stage of iodine dissociation which is critical for all following processes is starting just inside the upwind mixing layer, and so, the fluid dynamics of the layer is very important.

$$Re_x = \frac{32\sqrt{\gamma}}{(\gamma-1)^{3/4}(\gamma+1)^{5/4}} \left(1 + 2 \frac{T_\infty}{T_0}\right)^{-2} \frac{Re_a}{\sqrt{N}}; \quad (7)$$

$$Re_a = \frac{\rho_a u_a d_a}{\mu_a}; \quad N = \frac{P_0}{P_\infty}$$

Main parameter determining the flow mode in the supersonic jet is Re_x – Reynolds number based on the size of 1st cell (7). For typical N_2 -based low-pressure COIL $Re_x \sim 2000$ – correspond to the laminar flow mode [2]. Actually, in simulation [1] it has been shown, that the turbulent viscosity became significant in the interaction region only, where two opposite jets collide. It means that upwind BL of injected jet, as similar to free-jet BL, should be pure laminar up to collision area. After the initial coarse-grid simulation and two successive grid refinements numerically simulated upwind BL coincides well with theoretical curve [2] – see Fig. This refined grid was used for NS, RANS, LES, DES simulation – all these results are very similar. The standard kinetics package is used like in previous numerical model [1]. Multi-processor commercial code CFX-5 is used for massive-parallel computations.

In case of subsonic-mixing iodine injector [3] the Von-Karman-type vortex trail appears which is very similar to classical low-Reynolds oscillation in transversal cylinder flow. Instability originated in wake

behind the injected iodine jet. Frequency of the periodic oscillations is well matched with the theoretically estimated value $f=Sh \times U/d$, where $Sh \sim 0.3 \div 0.5$ is Strouhal number, U , d are characteristic velocity of incoming flow and characteristic scale. Such type of self-sustained oscillations exciting because of feedback-sensitive area of the flow is completely housed inside subsonic region where the feedback disturbances can go upstream.

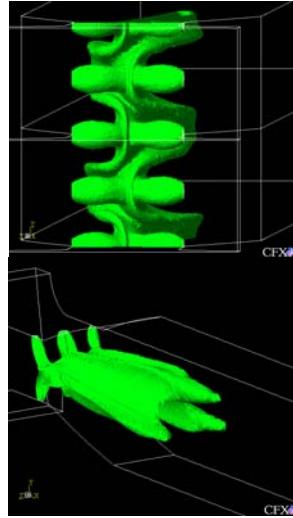


Fig. 12. Iso-surface of the I_2 concentration (50% level), view from the plenum chamber in the downstream direction.

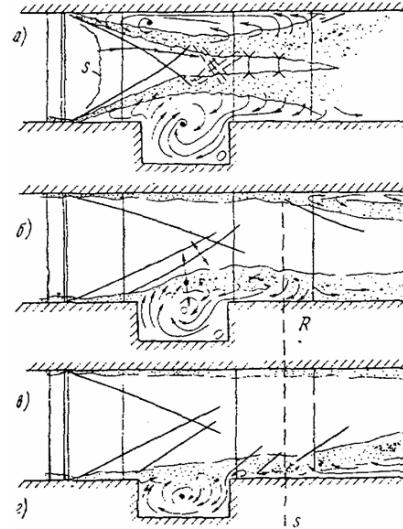


Fig. 13. Establishing of flow in laser cavity

In case of N_2 -based transonic-injection system the similar separated flow appears just after the injected jet. The feedback-sensitive part of flow is located in transonic and supersonic area, therefore disturbances cannot travel upstream and so the self-sustained periodic oscillations cannot be excited. Some small-scale chaotic oscillations remain because of instability of shear flow.

Another large-scale effect which is appears in transonic-injection system is the symmetry breakdown. In spite of perfectly symmetrical geometry of the domain and boundary conditions the flowfield tends to be essentially unsymmetrical (Fig 12). This non-symmetry is reflected in the local SSG distribution in the resonator cavity as well.

The main mechanism controlling the symmetry breakage down is Koanda effect in longitudinal vortex bands. The flow is essentially steady-state. Non-symmetrical structures cause increasing (doubling) of transversal scale δ and therefore second-degree decreasing of mixing rate:

$$m = \frac{1}{\tau_m} \sim \frac{\lambda}{\rho c \delta^2} \frac{Sc}{Pr}, \quad (8)$$

where λ , ρ , c are the fluid thermal conductivity, density and thermal capacity; δ is characteristic transversal scale; Sc , Pr are Schmidt and Prandtl numbers correspondingly. This effect is probably responsible for the over-estimation of SSG in early highly-symmetrical 3D simulations [1] $g_0/P \sim 0.22 \div 0.25 \text{ Torr}^{-1} \times \text{m}^{-1}$. The new optical axis-averaged SSG $g_0/P \sim 0.16 \div 0.18 \text{ Torr}^{-1} \times \text{m}^{-1}$ is much more consistent with measured values.

Therefore, NS-based thermodynamically-equilibrium universal-temperature model is verified and proved to be valid for the simulation of fluid dynamics and heat-mass transfer in iodine injector + cavity flow in spite of chemical reactions and electronic transitions. Simulation shows that for transonic nitrogen-based systems appears the large-scale symmetry breakdown which influences substantially on the mixing quality and finally on the lasing efficiency.

Cavity:

In this part of laser gas-dynamics circuit the processes of supersonic reacting streams interaction continue, moreover they pass in powerful electromagnetic field of laser radiation. In addition the preparation of laser medium flow to its discharge to the exhaust device (the pressure recovery system or the vacuum «cryosorber») finishes here.

The formation of laser beam taking account real characteristics of medium is probably one of the hardest problems of powerful gas lasers. The CFD methods in this case should be combined with the models of electromagnetic field. One of the problems of such kind of simulation lies in the fact that the character-

istic time of gas-dynamic and optical components of working process differs in several orders, whereas these components are joined strongly in energy way because of high temperature factor. It means that in complex simulation should be coordinated absolutely different requirements that are dictated by gas-dynamic processes having on the whole hyperbolic march nature and by optical processes having elliptic nature.

The optical character of radiation is determined substantially with the heterogeneities of active medium – with the refraction index as well as with gain. Special schemes of resonators that provide the indemnity of large-scale amplification heterogeneities of convection nature were developed for such mediums (Fig 13, 14).

Except of influence on radiation forming the heat-mass transfer processes determine the gas-dynamics of flow in many respects in this area, for example, the character of flow establishing. And it leads to practically important consequences. As an example the scheme of flow establishing in areas of resonator cavities will be examined. The vortex-type flow is formed in cavities [4] (Fig 13 a,b,c – step-by-step increasing of P_{00} – nozzle plenum pressure). Vortex sharply increases the thickness of the boundary layer, a reversed flow and separation zone are formed, and oscillations are often appeared. The supersonic flow after nozzle (Fig 13 b) is developing; however, the parameters of established flow are not yet realized here: P_{st} – static pressure is higher, and Mach number is lower than in case of normal laser operational mode. This is caused by thicker boundary layer, which becomes thicker as a result of back influence of separation flows (the forming of separation zone always results in the increasing of boundary layer thickness and P_{st} [5]). Finally the flow is established at further increasing P_{00} (Fig 13 c), when the further increasing P_{00} do not result in the changing of flow pattern, i.e. areas of disturbed boundary layer (disturbed by separation zone and gas ejection from cavity) are not changed practically. So when separation zones appear the character of channel start becomes asymptotic – P_{st} and Mach number reaches the design values gradually (as much as P_{00} increasing). And it is necessary to take in account when one chose the operation mode of laser. It is firstly.

Secondly, here the walls of channel are strongly heated because of higher heat-mass transfer. Stagnation temperature of flow, for example, for GDL is $T_0 > 1700K$, HF/DF-lasers have the same temperature. I.e. higher heat-mass transfer plays a negative role. They are fighting with it. It is possible to choose more optimal geometry of cavity, which decreases the intensity of shocks and oscillations; it is possible to organize the high-pressure cold air blowing up through small-size nozzles along the wall for decreasing of influence of separation zones. But the appearance is not removed completely, i.e. the task in specific channel demands of own solution.

Resonator:

Provision of resonator mirrors' efficiency requires upon high density of incident radiation the use of the most contemporary materials and technologies as well as of thermal-stressed processes simulation methods (Fig 16). As a result, nowadays it is possible to provide stable effective work of resonator without active cooling of mirrors even for the megawatt class lasers.

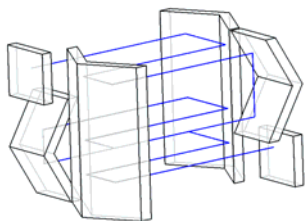


Fig. 14. HPL multi-pass resonator layout

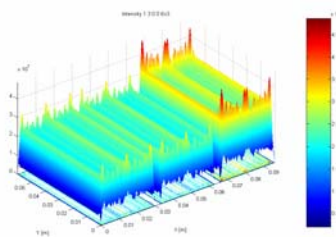


Fig. 15. Typical intensity distribution at the multi-pass resonator exit plane

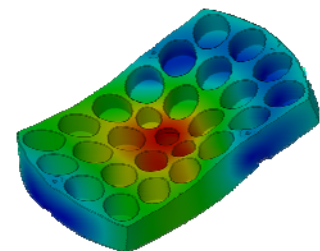


Fig. 16. HPL resonator mirror – thermal stresses and deformations

Diffuser:

The principal mission of the diffuser is a maximum effective transformation of kinetic energy of exhausted laser medium's supersonic flow. This mission becomes more complicated because of incompleteness of physicochemical and relaxation processes in the flow in the resonator cavity, and it leads to considerable heat generation. Also it becomes complicated because of small Reynolds numbers ($\leq 10^4$). In this condition the viscous-inviscid interaction that determines the effectiveness of pressure recovery in diffuser differs from classical one appreciably. The magnitude of heat generation in COIL diffuser depends strongly on the effectiveness of laser radiation, and the corresponding temperature factor may vary

within the wide range: $1.5 \leq \theta \leq 2.5$ during the working cycle of laser. Especially strong influence of thermal effects is exerted upon boundary layer (Fig. 17), therefore heat exchanging processes on the walls influence strongly the effectiveness of diffusers' work. The use of mostly contemporary approaches to designing and simulation, the use of new active methods of boundary layers control are the dominant factors that provide high technical characteristics of the entire laser.

Supersonic diffuser of any chemical laser has considerable difference from typical air-dynamic wind tunnel diffuser. The flow is much more complex due to the presence of the following features: (1) elongated rectangular cross-section; (2) vanes separating the whole cross-section; (3) mirror cavities; (4) boosters, shutters and others. Due to those distinctions the complex under-start behavior appears during the laser operation [6, 7]. In COIL diffusers all these phenomena appear as well. Additionally the viscous-induced and thermal-induced features appears. All these features cause reducing of the diffuser efficiency; therefore, the main goal of the investigation is maximizing of the diffuser efficiency and minimizing influence of the mentioned factors.

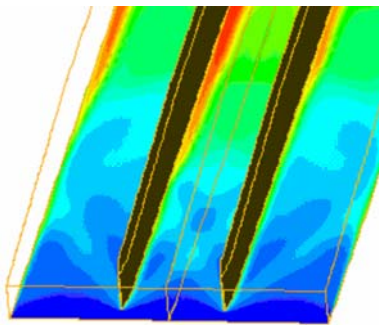


Fig. 17. Numerical simulation of high-q diffuser 3D turbulent flow

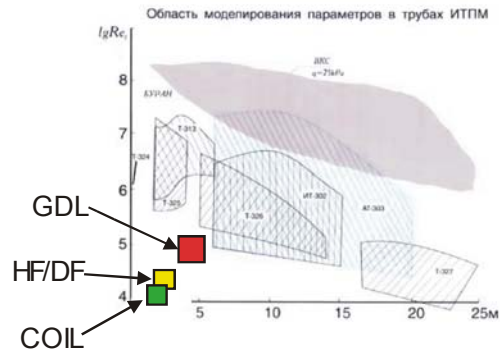


Fig. 18. Gas-dynamic parameters of air-dynamic wind tunnels and supersonic gas lasers

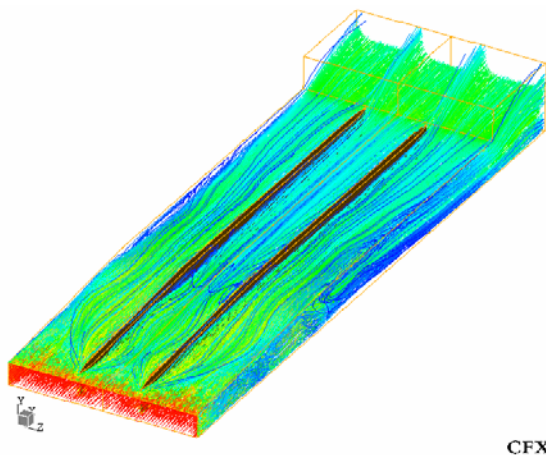


Fig. 19. Three-dimensional near-wall structure of flow in supersonic diffuser channel, RANS $k-\omega$ SST simulation

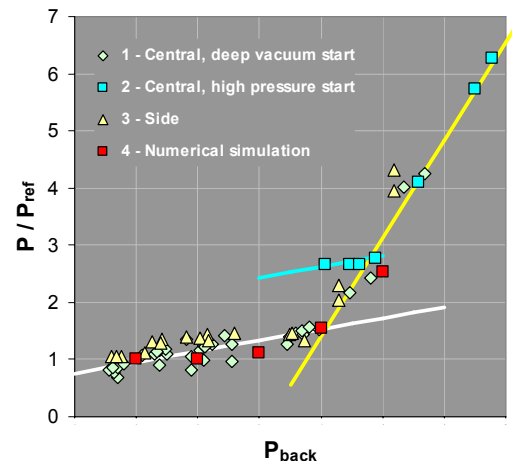


Fig. 20. Resonator cavity pressure vs. backpressure: 1, 2, 3 – 15-kW COIL measurements; 4 - 3D RANS $k-\omega$ SST simulation; solid line – normal start approximation; dashed line – unstart approximation.

Reynolds numbers for COIL SD flows lie in range $10^3 \div 10^4$. RANS numerical simulation based on $k-\omega$ SST model show that even in case of zero heat release there is considerable influence of viscous dissipation on the diffuser efficiency below $Re \sim 10^4$.

The simplified integral-based analysis is very useful for rough initial estimations. Certainly it is not enough for deep understanding of flow structures. 3D RANS based on $k-\omega$ SST model with standard kinetic package like in [1] is proved to be valid for the COIL diffuser simulation. Verification procedure is based on the two approaches: (1) grid convergence and (2) comparison with real 15-kW COIL experiments [1]. Unstructured grid adapted to the flow structure and refined in high-gradient areas allows getting of grid-converged solution. Simulated wall pressure profile along the downstream direction compared with experimental data measured on 15-kW COIL diffuser is shown in Figs 21. Comparison exhibits good overall quantitative coincidence as well as detailed shape of the curve.

As long as the 3D numerical model has been verified experimentally, details of the flowfield can be investigated numerically. For example, characteristic local maximum on the pressure profile appeared in

experiment (Fig. 22, points) as well as in simulation (solid line) is caused by interaction of vane-induced shock waves followed by the rarefaction wave.

Because of boundary layers (BL) in COIL diffusers are very thick due to viscous and thermal effects right the BLs growing up, laminar-turbulent transition and separation limiting the whole diffuser performance and efficiency. Boundary layers on the channel walls are initially laminar under the typical conditions of nitrogen-based low-pressure COIL (Fig. 17). The first shock incidence leads to sudden thickening of BL, whereas the second one causes pronounced turbulent transition. All this behavior appears in three dimensions. Because the fluid in BLs is almost completely quenched due to wall influence as well as due to big local residence time, the total translational temperature in near-wall area is very close to equilibrium temperature $\sim \theta \times T_{0-in}$. This factor causes the thermal-induced entropy rising and the total pressure dropping in BLs and further – very high sensitivity to any positive pressure gradient in downstream direction. Probably just the thermal effects in BLs limit the potential efficiency of the diffuser.

Experimental measurements of the static pressure before the COIL diffuser during lasing backpressure tests are shown in Fig. 20 along with simulated data. All data show that the diffusers unstart is smoothed unlike to DF lasers unstart [6].

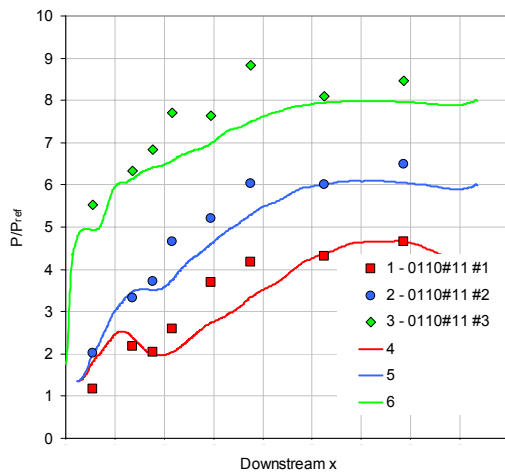


Fig. 21. Experimental wall pressure for three different backpressure level (1, 2, 3) measured in laser experiments on 15-kW COIL; corresponding simulated wall pressure downstream profiles (k- ω SST RANS).

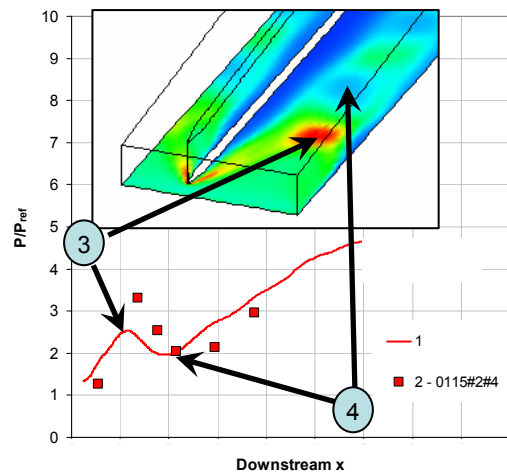


Fig. 22. Wall pressure profile and flow structure details: 1 – 3D RANS k- ω SST simulation; 2 – 15-kW COIL measurements; 3 – shock waves interaction; 4 – expansion waves interaction.

The following methods are used in gas dynamics for boundary layer control: either the suction of boundary layer, or the blowing up of high-pressure gas from small-scale nozzles directly in area of a low-pressure boundary layer (thus a boundary layer velocity profile is made more filled and, accordingly, the effective thickness of boundary layer is reduced, and the probability of boundary layer separation is reduced too).

In case of COIL diffusers it is expedient to make the gas injection right after laser cavity in the beginning of diffuser. Thus it is possible to reduce also a negative effect of heat generation. As in case of COIL PRS it is necessary to use two-stage ejector (because a PRS should supply the compression ration of flow about 70-90) there is a capability to combine a gas injection along walls with the role of ejector first stage. The concept of active diffuser is consisting in it. The active diffuser plays a role of the ejector first stage.

However if the injection of high-pressure gas is organized only along walls, it is impossible to receive effective ejection of low-pressure laser gas. Because a ratio of active nozzle area and laser channel area is far from optimum. Thus, there is a task of choice of injection unit geometry with the purpose of organization of effective mixing of two flows, i.e. it is the task of mass transfer.

As multi-section diffusers are used in lasers (i.e. the rectangular cross-section channel is divided on section by pylons) the solution of task is obviously enough: to use short pylons as additional injection device for active gas supply. In this case supersonic jets behind short pylons will play a role of walls (liquid walls) and thus multi-sectional design of channel will be kept, and the ratio of active and passive areas will improve. At the same time it is clear, that the task of mixing is determined by very large number of parameters: not only choosing of injection unit geometry, geometry of nozzles, angles of injection, but also choosing of gas parameters, definition of mixing chamber geometry etc.

The experimental determination of working parameter area of effective operation of such active diffuser is impossible. It is possible to rely on three-dimensional numerical simulation of flow only, using, for example, such packages as CFX. But given task of mixing is difficult enough. It is necessary to solve the problem of simulation of input flow into the diffuser – first of all it should have a heat generation process in a flow. In an ideal case it is necessary to take into account a flow pattern after COIL multi-nozzle bank where reacting components of laser gas mix up. The simulation procedure should be verified. As a result of verification one should choose the suitable model of turbulence, choose the type and detentions of grids, one should check up the stability of solution and etc. For verification procedure the model experiments usually are necessary.

The example of simulation of a flow field in the active diffuser is shown on Fig. 23: fields of pressure are shown, the sonic line is marked. Experimental and simulated distribution of P_{st} along a channel of active diffuser at different back pressure (Fig. 25) exhibits good agreement. Realization of regular parametric calculations when main parameters are varied, allows determining area of parameters which is the most suitable for the solution of task - reaching the maximum pressure recovery after diffuser. The active diffuser realized for COIL of 10 kW class is shown on Fig. 24.

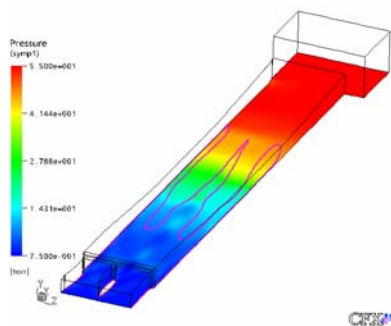


Fig. 23. Flow field in active diffuser



Fig. 24. Active diffuser

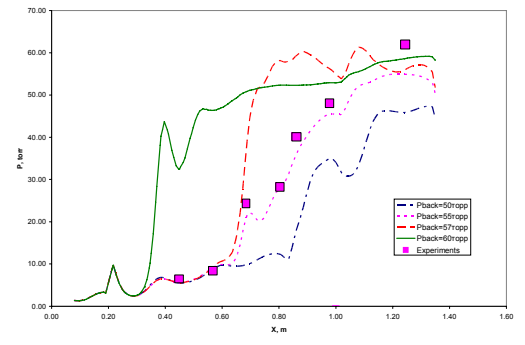


Fig. 25. Wall pressure curves – simulation and experiment

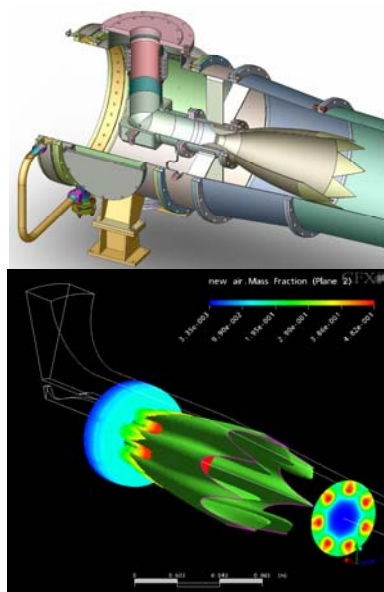


Fig. 26. HPL PRS ejector flows

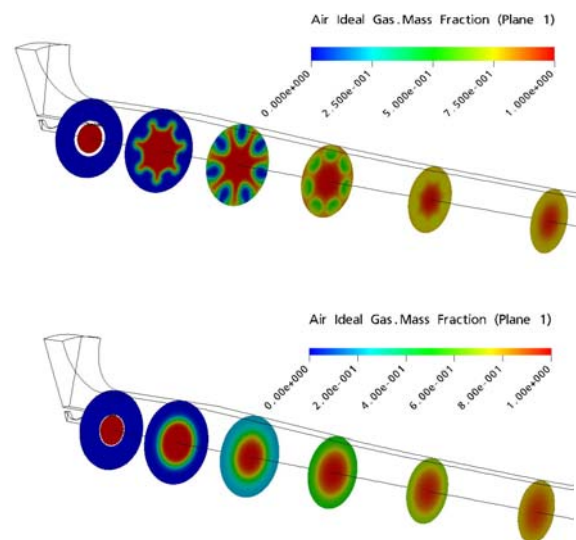


Fig. 27. Flow fields in ejector mixing chambers of different design

Ejector:

Because of low density of laser medium and high heat release in diffusers, the coefficients of ejection in contemporary pressure recovery system of supersonic chemical lasers are small enough; therefore size and weight of ejectors determine size and weight of the entire laser system. Therefore the understanding of the processes in these devices determines the technical level and the competitive ability of the entire laser system noticeably.

High temperature combustion products are used as an active gas for the increasing of the ejection coefficient. The processes of turbulent heat-and-mass transfer between active and passive mediums that have different molecular weights and temperature (temperature factor $\theta=T_{01}/T_{02}\sim 3..4$) takes place in laser ejection.

tors. The use of untraditional schemes of nozzle devices that provide the intensification of mixing is necessary for the provision of high effectiveness of ejector working process $\eta = \varepsilon n$ ($\varepsilon \sim 10..100$ – compression degree, n – ejection coefficient) - Fig. 26.

Different type muzzles on ejector nozzle – as passive devices – and injection of small-size jets on the certain angle to flow – as active devices – are possible to use as devices for intensification of mixing processes of ejected and ejecting flows (the injectors of ejecting gas is located on ejector nozzle outlet also). The general idea of such approach is clear – to increase the mixing surface and to form the vortex motion of one gases relatively another one. At the same time, how to choose the specific parameters and geometry of such devices – is not a simple task. The fact is that the number of parameters is big in the task: number of elements intensifying mixing, the shape and dimensions of elements, the inclination angle of element to flow and so on. And efficiency of ejector (ejection coefficient and compression ratio) depends on how successfully these specific parameters were chosen. It is clear, that such task can not be solved experimentally only. The using of modern tools of computational modeling of viscous 3D-flow (as in case of active diffuser) allows to solve this problem. The series of parametric calculations is carried out, i.e. all parameters of these elements are varied, and area of optimal parameters is determined on the base of computing results of ejection coefficient for specific geometry. The results of flow calculation for one variant of passive intensifier – muzzle on nozzle, so called “chevron” (three-angle plates continuing the ejector nozzle) – are shown on Fig 27.

The flow pattern after usual nozzle and nozzle with 7 chevrons are compared on fig. 27. Evidently how the mixing surface after such device is increased. Evidently how the mixing process is developed, and mixing intensification is occurred due to development of vortex structure of flow.

Introducing the quantity characteristics of flow: dispersion of next value $D_{\mu} = \sqrt{D} / (MO_1 + MO_2)$ (where

$MO = (\iint_S M dS) / S$ - average of distribution of variable M , $D = (\iint_S (M - MO(M))^2 dS) / S$ - dispersion of

variable M , S – sectional area, $M = \rho \times v$ and $M = \rho \times v^2$) it is possible to compare quantitatively different design solution from point of view of mixing efficiency. The mixing is more intensive in case of using of chevrons, i.e. mixing process is finished early. On base of such results it is possible to correct the geometry of mixing chamber - it can be made shorter in case of chevrons.

Successful solution of similar task – actually task of mass transfer – allows improving the ejector characteristics on 30-35%. It is a very important result. The ejectors are used in pressure recovery systems for supersonic chemical lasers, and they determine in many respects the mass-dimensional characteristics of laser complexes, because the whole weight of complex is determined by component storage system for gas-generator supplying ejector. Improving of ejector characteristics means decreasing mass-dimension characteristics of whole complex.

Thus the processes of heat-mass transfer are the base of working processes of contemporary high power chemical lasers, and their perfecting is one of the principal factors upon the creation of effective laser systems.

1. Boreysho A.S, Barkan A.B., Vasil'ev D.N., Evdokimov I.M., Savin A.V., QUANTUM ELECTRON, 2005, 35 (6), 495-503.
2. V.S. Avduevsky et al, Gas dynamics of supersonic non-isobaric jets, M., Mashinostroenie, 1989 (in Russian).
3. Madden T.J. Proc. SPIE, 5120, 363-375 (2002).
4. N.A. Shushin. Experimental investigation of start of rectangular air dynamic wind tunnels with the cavity in test section and gas blowing up in diffuser. Proceeding TSAGI №2208, 1984.
5. G.N. Abramovich. Applied gas dynamics. Published by “Science”, Moscow, 1969.
6. Boreysho A.S., Malkov V.M., Start features of Supersonic Chemical Laser (SCL) channel, operating with Pressure Recovery System (PRS), GCL-HPL-2006.
7. Malkov V.M, Boreisho A.S., Savin A.V. et al., About the choice of working parameters of pressure recovery systems of supersonic chemical lasers, Thermophysics and Aeromechanics, v.8, № 4, p.589-600, 2001.
8. Alexeev K.O., Druzhinin S.L., Evdokimov I.M., Savin A.V., Trilis A.V., Three-dimensional flow structures in counter-flow jet SOG, GCL-HPL-2006.